

Supplementary Information

Design of Iso-material Heterostructures of TiO₂ via seed mediated growth and arrested phase transitions

Deb Sankar De^{§ †}, Dilip Kumar Behara^{§†}, Sulay Saha^{§†}, Arun Kumar^{*}, Anandh Subramaniam^{**}, Sri Sivakumar^{§‡\$*}, and Raj Ganesh S Pala^{§†*}

§Department of Chemical Engineering, Indian Institute of Technology Kanpur

‡Material Science Programme, Indian Institute of Technology Kanpur

Department of Physics, J.C. Bose University of Science and Technology YMCA, Faridabad-121006

§Centre for Environmental Science & Engineering, Thematic Unit of Excellence on Soft Nanofabrication, Indian Institute of Technology Kanpur, Kanpur, UP-208016, India

** Material Science Engineering, Indian Institute of Technology Kanpur*

** Corresponding Authors: anandh@iitk.ac.in, srisiva@iitk.ac.in, rpala@iitk.ac.in*

† Equally Contributed

S1.1. Lattice parameter estimation of Anatase and Rutile TiO₂ from DFT and DFTB

The crystalline structure of TiO₂ is tetragonal for both rutile and anatase phase with each Ti atom is coordinated with six neighboring O atoms situated at the vertices of a distorted octahedron. The calculated lattice parameter values ($a=b$ and c) matches well with the experimental lattice constant values. In bulk crystalline structure of TiO₂ (rutile and anatase), there exists two types of bonds between Ti and O atoms; one of them is elongated in comparison to other. The bond length in longer type is 1.98 Å in both anatase and rutile phases, whereas the bond length in case of shorter type is 1.93 Å for anatase while it is 1.95 Å for rutile phase of TiO₂ (Figure S1). Anatase and rutile clusters are constructed out of these bulk structures in a stoichiometric way (Figure S2). After structural relaxation, if Ti-O interatomic distance is less than 2.1 Å, then we can assume that the bond formation has occurred.

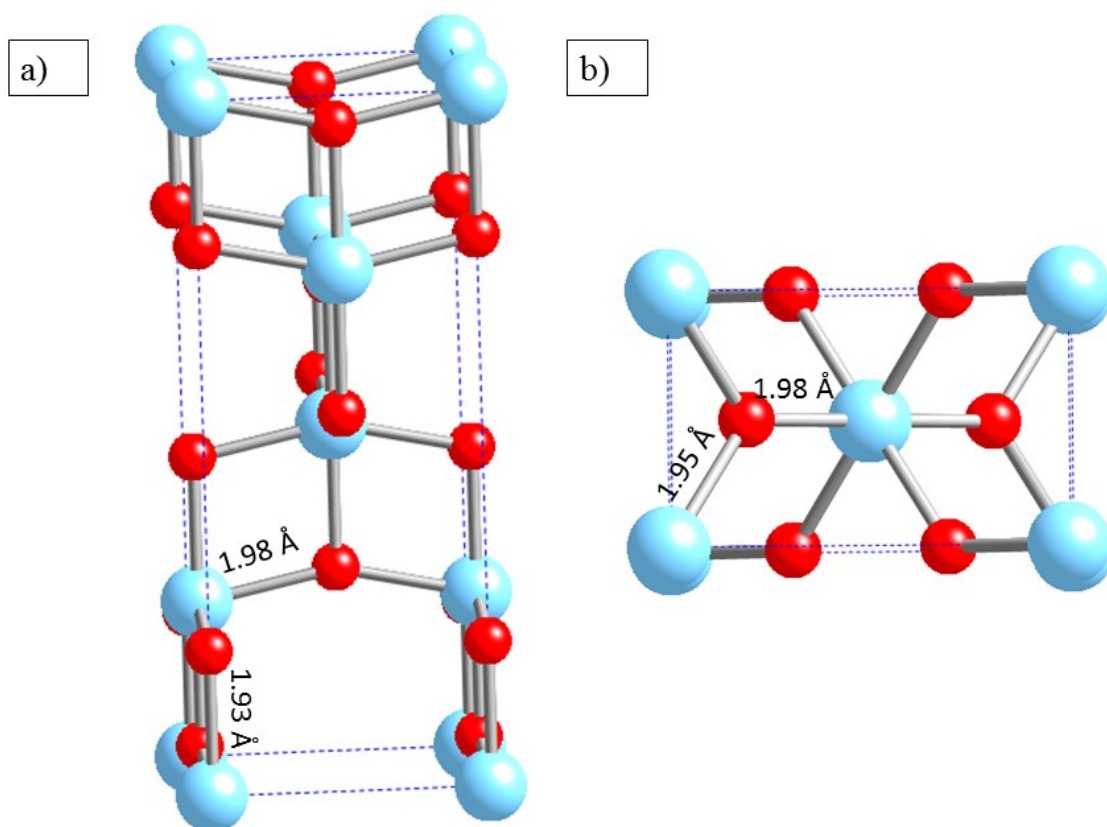


Figure S1: Two types of bond lengths in a) anatase TiO₂ and b) rutile TiO₂ clusters

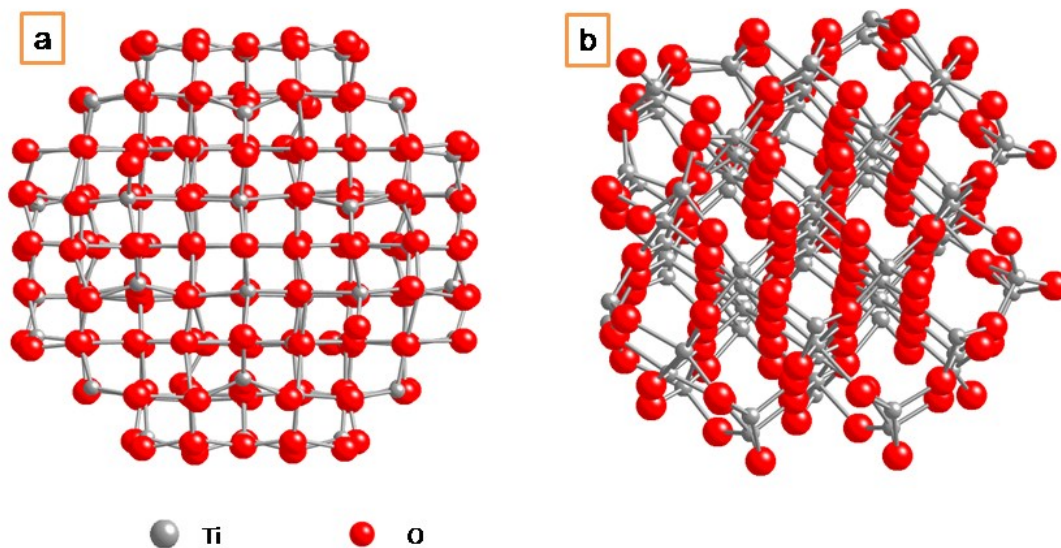


Figure S2. a) Anatase a) Rutile clusters used for computational calculations

S1.2 Stability of anatase and rutile TiO₂: cluster size dependence

Energetics of different spherical clusters of (TiO₂)_n, for different n, (where n = number of formula units) were calculated (Figure S3). The results suggest that for n < 12 formula units, anatase cluster is more stable than the rutile cluster. Further, we can observe that till 12 formula units there is no bulk contribution for the cluster and anatase TiO₂ becomes more stable. We observed that appropriate sub-surface and surface region is absent in clusters of n < 12 f.u. Hence, the surface energy determines the stability order in the polymorphs and anatase is found to be more stable. However, after 12 formula units, the bulk energy contribution dominates and the cluster reaches to a structure that is more close to bulk.

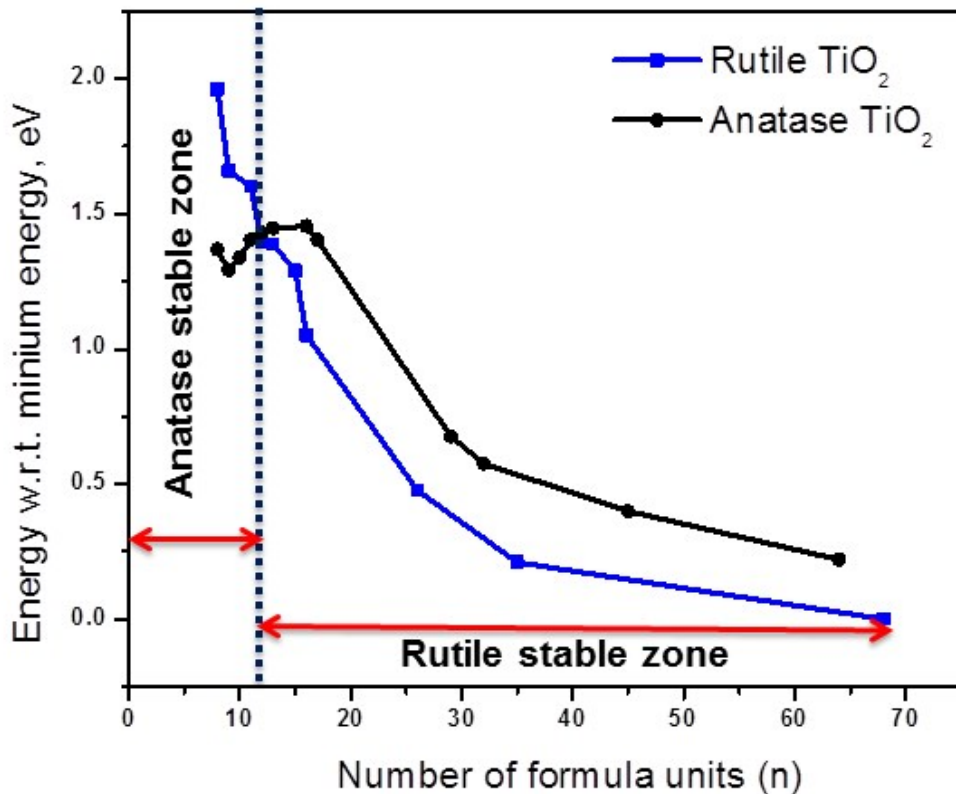


Figure S3. Normalized energy vs. number of formula units demarcating the stability zones of anatase and rutile clusters.

In all computations, it has been assumed that cluster is spherical whereas experimentally different morphologies have also been observed¹⁻³. From our calculations, it has been observed that anatase phase is more stable than rutile phase in lower dimensional regime which supports very early experimental report of Banfield *et. al.*⁴ They confirmed the reversal of phase stability for anatase and rutile TiO₂ at around 14 nm particle size. Since, the bulk contribution to total energy is insignificant below 12 f.u., as evident from single phase cluster analysis, all the computations pertaining to heterostructures have been done for more than 12 f.u. units.

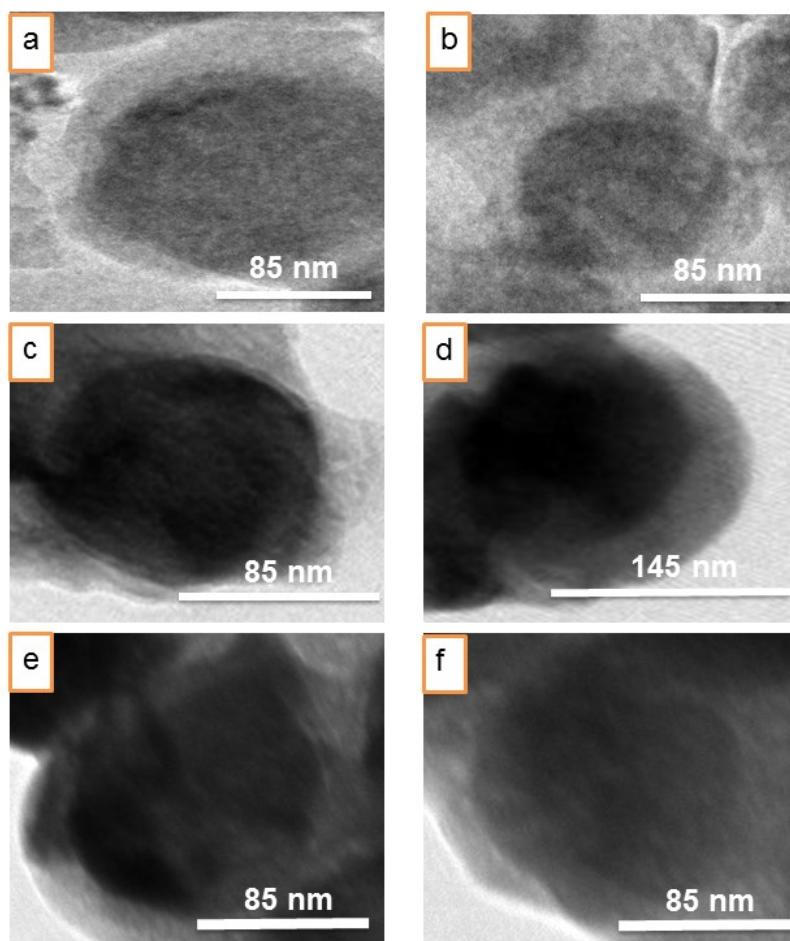


Figure S4. Representative TEM images of rutile/N-anatase/NN TiO₂ *iso*-material heterostructure formed in core-shell form (a to f).

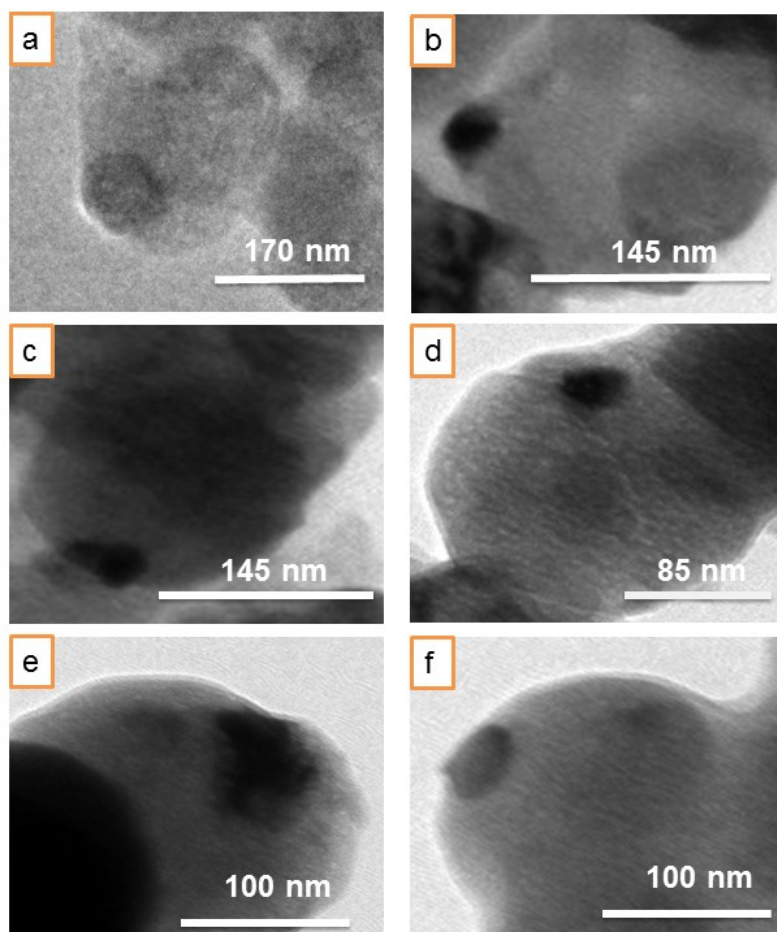


Figure S5. Representative TEM images of rutile/N-anatase/NN TiO₂ *iso*-material heterostructure formed in yolk-shell/Janus form (a to f)

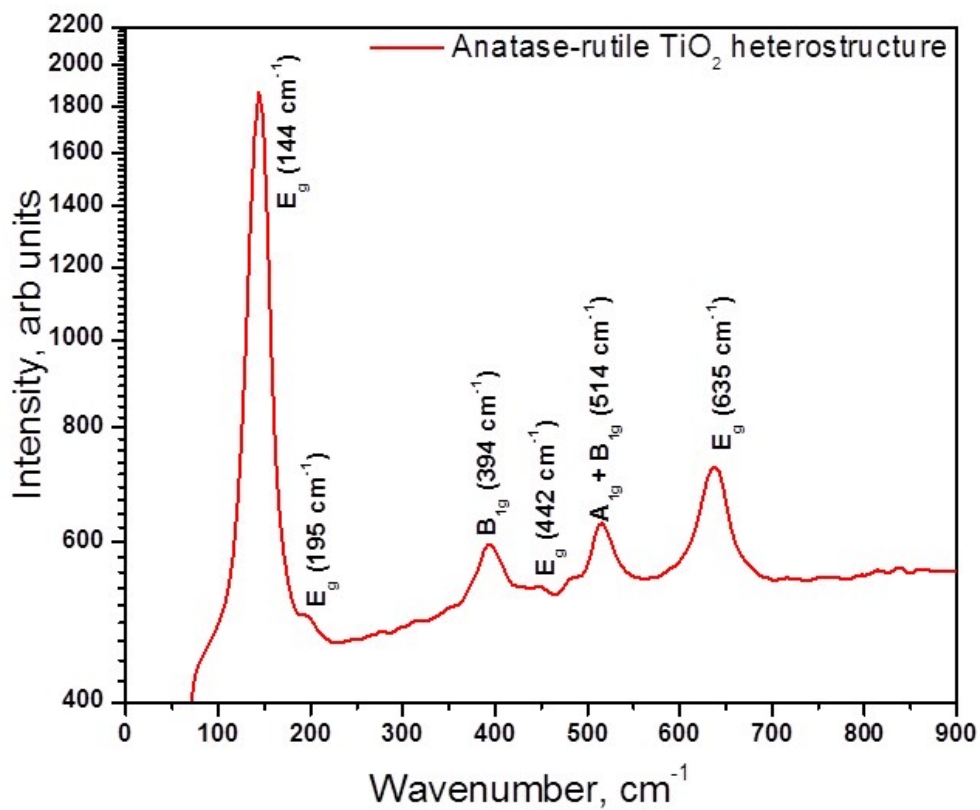


Figure S6. Raman spectra of rutile/N-anatase/NN *iso*-material TiO_2 heterostructure.

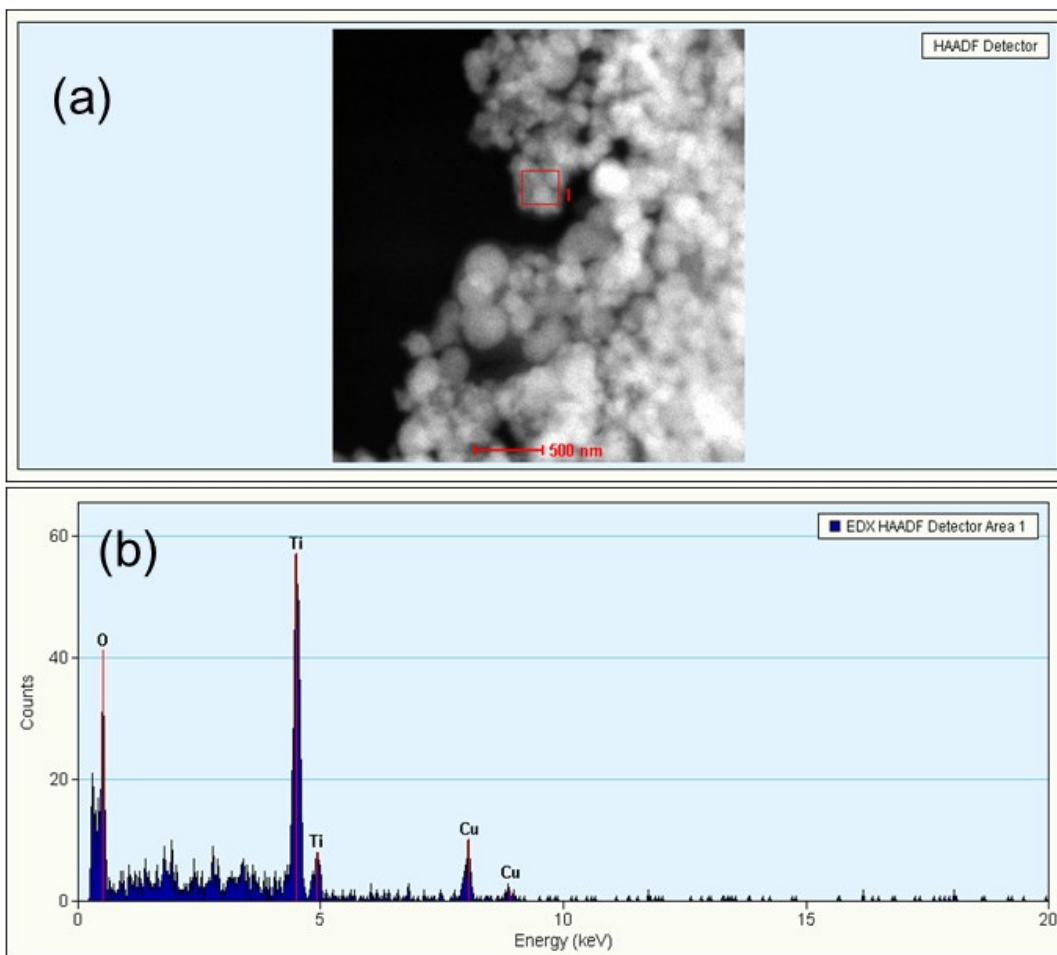


Figure S7. STEM-HAADF spectrum of rutile/N-anatase/NN TiO₂ *iso*-material heterostructure; a) TEM image, and b) corresponding elemental mapping

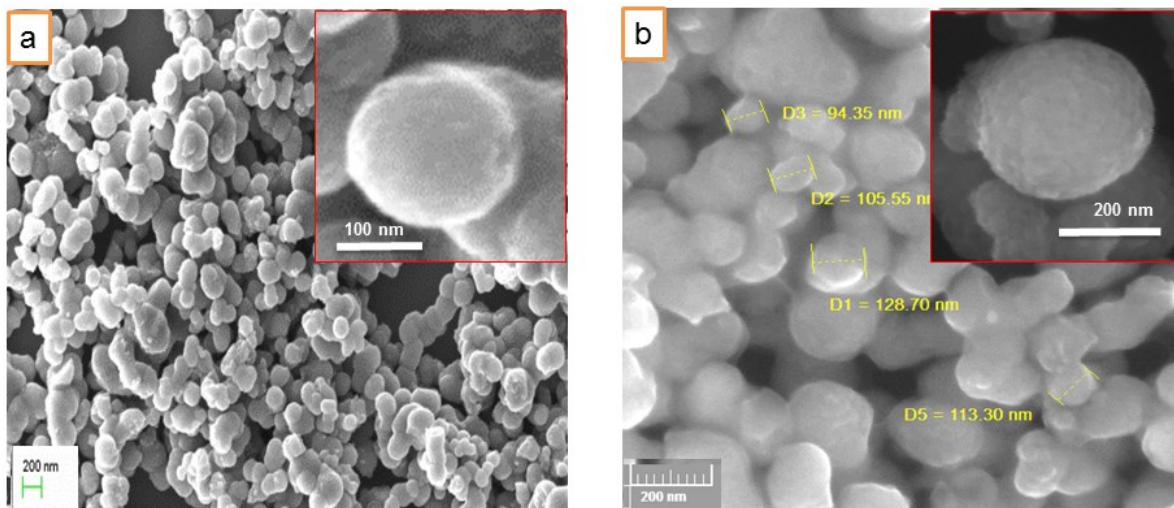


Figure S8. SEM images of (a) rutile/N TiO₂ and (b) rutile/N-anatase/NN TiO₂ heterostructure morphologies (Inset SEM images are taken at higher magnification).

S1.3. Interface dependent Janus structure

It is observed from computational calculations that the interface plays a major role in the structural stability and phase transformation pathways. The unsaturated bonds at the surface and the interface will determine the stability of the heterostructure. Depending on the material composition, structure and contact between the phases, there can be different type of interfaces (Janus/yolk-shell) can be observed. Among different Janus type *iso*-material heterostructures, we considered few configurations consisting 80% anatase and 20% rutile for stability calculations. The energy for stable and unstable configuration is shown in Figure S9. For these interface calculations, FigureS9-i is taken as reference energy state for all other heterostructure combinations. The calculated energies suggest that structures with a smaller number of unsaturated bonds at the interface will tend to make more stable and more under coordinated/unsaturated bonds always try to destabilize the system. Figure S9-iv to S9-vi have a greater number of unsaturated bonds at the interface than the Figure S9-i, S9-ii and S9-iii which leads to Figure S9-iv, S9-v and S9-vi to a less stable configuration. Among all the heterostructure combinations, Figure S9-i is considered for energy landscape calculations.

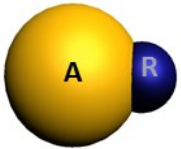
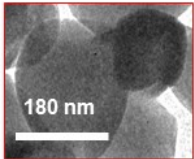
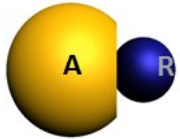
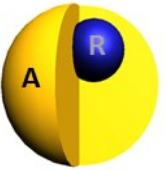
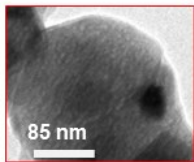
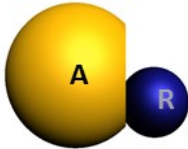
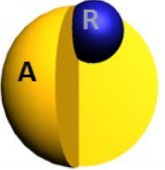
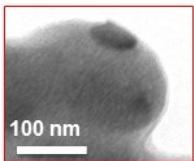
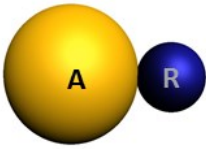
Stable configurations			Unstable configurations		
Heterostructure	Observed TEM image	Energy, eV	Heterostructure	Observed TEM image	Energy, eV
(i) 		0	(iv) 	—	0.24
(ii) 		-0.08	(v) 	—	0.56
(iii) 		0.03	(vi) 	—	0.56

Figure S9. Schematic representation, energy values and observed TEM images of different computationally developed stable and unstable rutile/N-anatase/NN *iso*-material TiO₂ (yolk-shell/Janus) heterostructures.

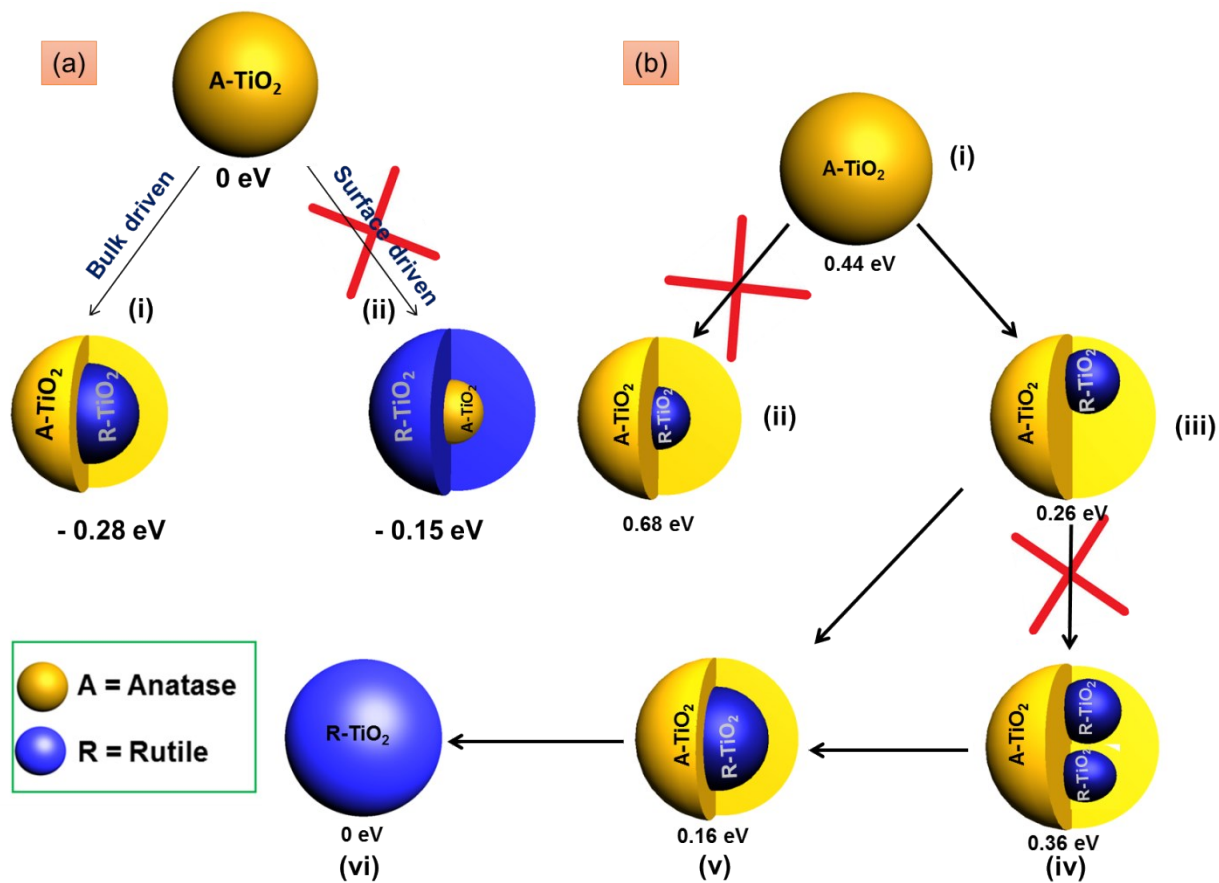


Figure S10. a) Schematic representation of anatase to rutile phase transformation based on 230 formula unit calculation: i) bulk driven path, and ii) surface driven path; b) Mechanism for bulk driven anatase to rutile TiO₂ transformation based on 230 formula units.

S1.4. Electronic structure of bulk lattice, clusters and heterostructures:

All the heterostructure clusters having 230 f.u. are found to behave like metal on account of increased under coordination at the interface (Figure S13). The findings are in stark contrast to the experimental results of iso-material TiO₂ heterostructures, wherein a bandgap has been observed. The discrepancy can be accounted by the fact that the considered theoretical clusters are smaller than the heterostructures studied experimentally, resulting in a greater concentration of mid-gap states. Furthermore, the surface atoms of a heterostructure are partially/fully saturated in experiments, which are not reflected in the theoretical calculations.

The Janus heterostructures have lower under coordination in comparison to core-shell heterostructure. A thin layer of shell in the core-shell heterostructure (i.e. larger interface) has greater number of under coordination in comparison to a heterostructure having thick layer of shell in the core-shell heterostructure (i.e. small core). The Yolk shell heterostructure has the maximum under coordination among the heterostructures. The presence of under coordinated atoms generates new electronic states near the Fermi level (Fig SI 13).

Table S1. The weighed percentage of different Ti-atoms (i.e. different co-ordination numbers) in different TiO₂ clusters and iso-material heterostructures. The maximum Ti-O bond distance is considered to be 2.25 Å.

	Ti-6c*	Ti-5c*	Ti-4c*	Ti-3c*
Anatase/NN cluster	60	16	13	8
Rutile/N cluster	64	16	8	10
Anatase(small)/NN(core)-Rutile(large)/N(shell)	42	43	13	2
Rutile(small)/N(core)-Anatase(large)/NN(shell)	37	33	20	10
Rutile(large)/N(core)-Anatase(small)/NN(shell)	32	42	18	8
Janus: Anatase/NN(20%)-Rutile/N(80%)	51	26	11	12
Janus: Anatase/NN(80%)-Rutile/N(20%)	55	16	16	13
Yolk: Anatase/NN(80%)-Rutile/N(20%)	45	24	17	14

*where Ti-nc corresponds to a Ti-atom having a co-ordination number of n.

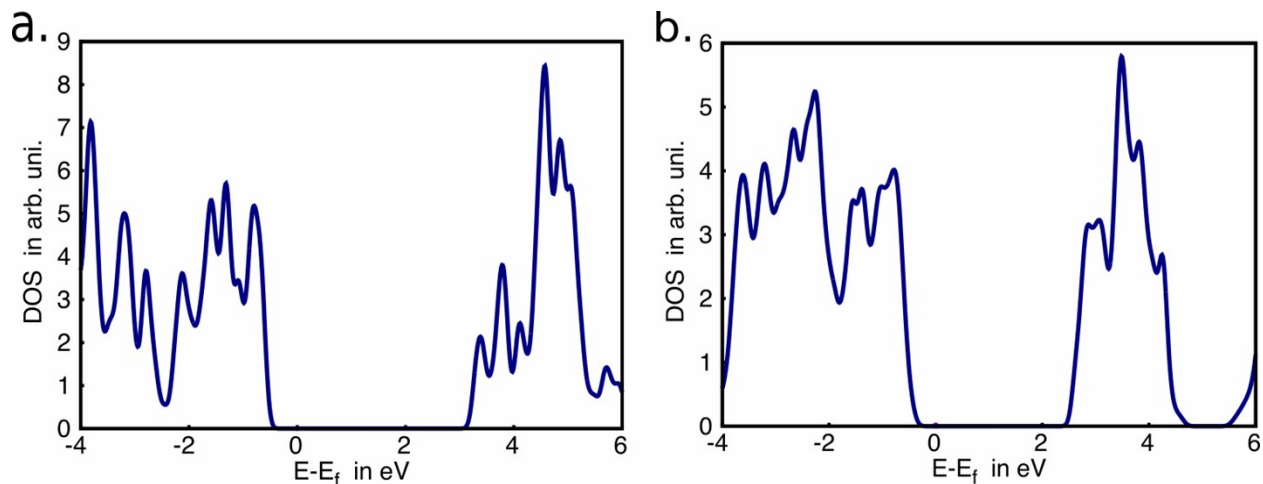


Figure S11. Total DOS of bulk lattice structure of (a) Anatase/NN (3.3 eV) and (b) Rutile/N (2.8 eV).

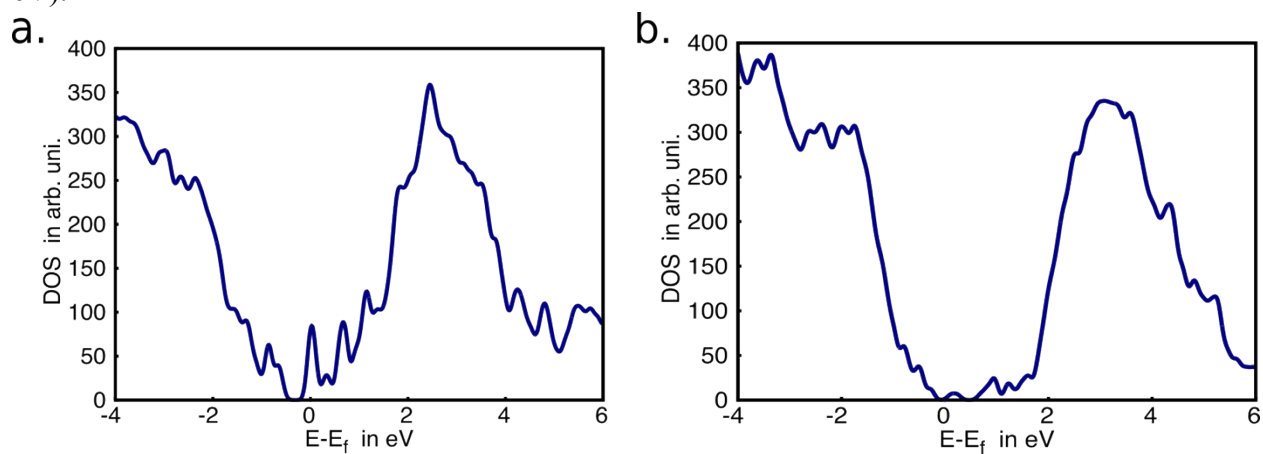


Figure S12. Total DOS of (a) Anatase/NN and (b) Rutile/N cluster comprising 230 f.u.

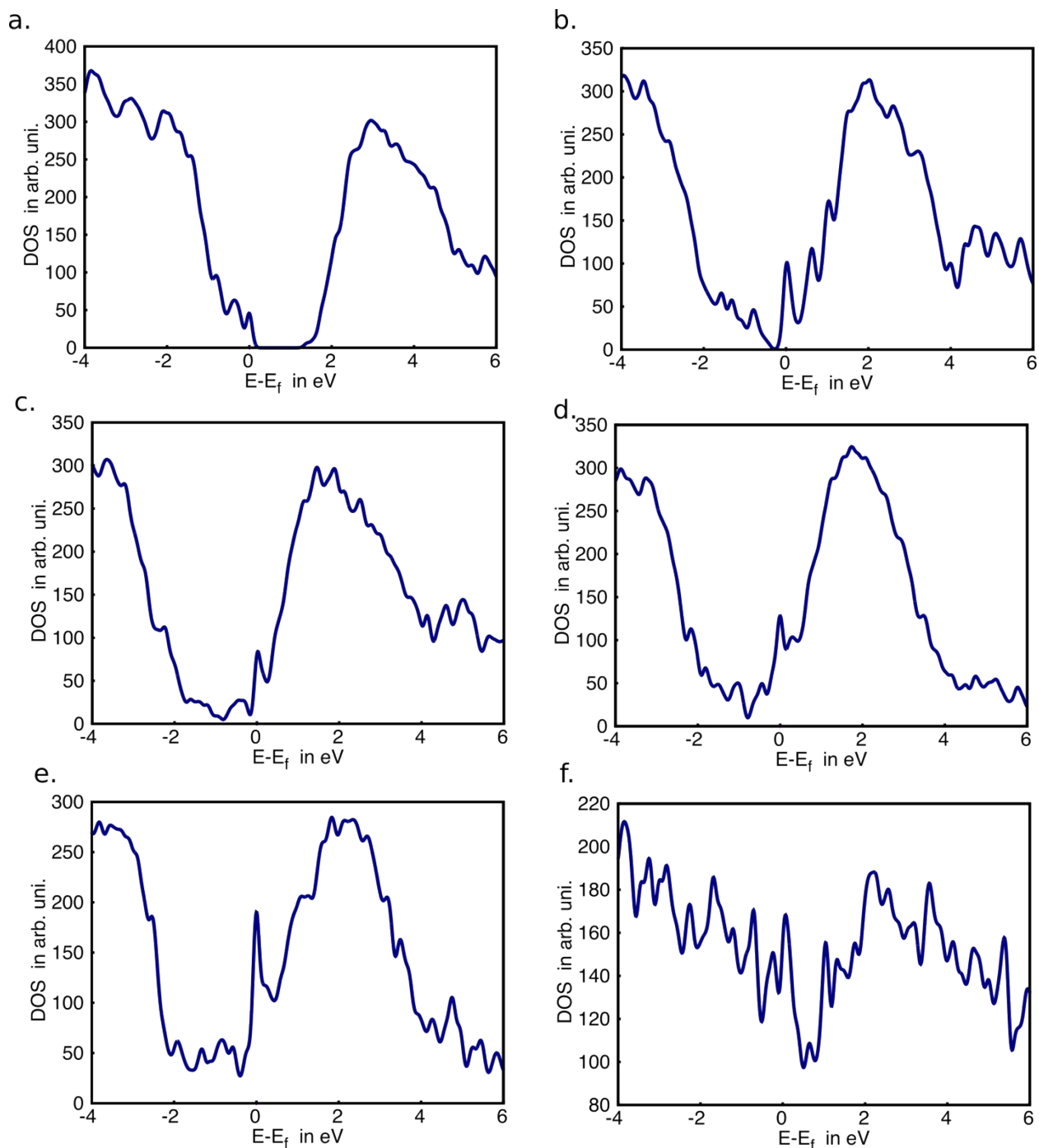


Figure S13. Total DOS of heterostructures having (a) Anatase(small)/NN(core)-Rutile(large)/N(shell), (b) Rutile(small)/N(core)-Anatase(large)/NN(shell), (c) Rutile(large)/N(core)-Anatase(small)/NN(shell), (d) Janus: Anatase/NN(20%)-Rutile/N(80%), (e) Anatase/NN and (f) Janus: Anatase/NN(80%)-Rutile/N(20%), and (f) Janus: Anatase/NN(20%)-Rutile/N(80%) cluster comprising 230 f.u.

S2. Detailed finite element methodology

Figure S14 shows schematics of the 3-dimensional finite element models (cut-section) used for the simulation of the stress state of: (a) core-shell and yolk heterostructures and (b) Janus heterostructures. In part (a), the ' r_0 ' and ' r_i ' represents the outer and inner radius values respectively and, ' d ' represents the displacement of core center (C_2) with respect to shell center (C_1). For the core-shell heterostructure, the value of ' d ' is set to zero and for yolk structures, ' d ' has finite values in the range $0 < d < (r_0 - r_i)$. In part (b), for Janus heterostructure, there is one radius value represented with r_0 (as for determination of stability, same total volume of the various heterostructures has been assumed, giving the same values for outer radius in core-shell/yolk structures and radius of spherical half domains in Janus structure). Also the centers of two half domains coincide in case of Janus structure. It is also important to note that the values of r_0 and r_i are computed such that the volume of two phases: Rutile/N and Anatase/NN (core and shell in part (a) and two spherical half domains in part (b) of the figure) are equal. In both the models, the displacement boundary conditions are used. The centre C_1 of the domains is locked in x-, y- and z-directions (pinned boundary condition at C_1). The lattice mismatch strain of 3.6% at the interface, is imposed as thermal strains in the regions highlighted with blue color (marked as Region-A in the figure). The misfit strain (eigen-strain) is fed in an isotropic manner in the shell for core-shell and yolk morphologies and in biaxial manner in rutile phase for Janus heterostructure. The domains are meshed with tetragonal elements (C3D6R type elements) with uniform mesh size of 0.2nm and the numerical domains are simulated using commercially available ABAQUS 6.11 software.

The strain energy (SE) are computed for various values of r_0 (and thus r_i in core-shell and yolk heterostructures) using finite element method (FEM). For each heterostructure, the values of SE are compared with interfacial energy (IE) for various values of r_0 , to determine the critical size (r_C) for stability of coherent and incoherent interface. The value of r_C can be obtained by computing the size (r_0) of the domain, wherein, the total energy for domains with incoherent interface (E_{In}) becomes lower than that with coherent interface (E_C) for $r_0 > r_C$. The contribution of bulk energy and relevant surface energy for the computation of E_C and E_{In} , is additive in nature, thus shifts the curve along y-axis and will have no effect on the r_C . Also, the total energy (E_{total}) for all various heterostructures are computed and compared, at three different length scales: angstrom regime, nano-regime and micro-regime, to determine the stability of different

morphologies. The E_{total} has been computed by adding the bulk free energy, relevant surface energy, strain energy for sizes $r_0 < r_C$ and interface energy for sizes $r_0 > r_C$.

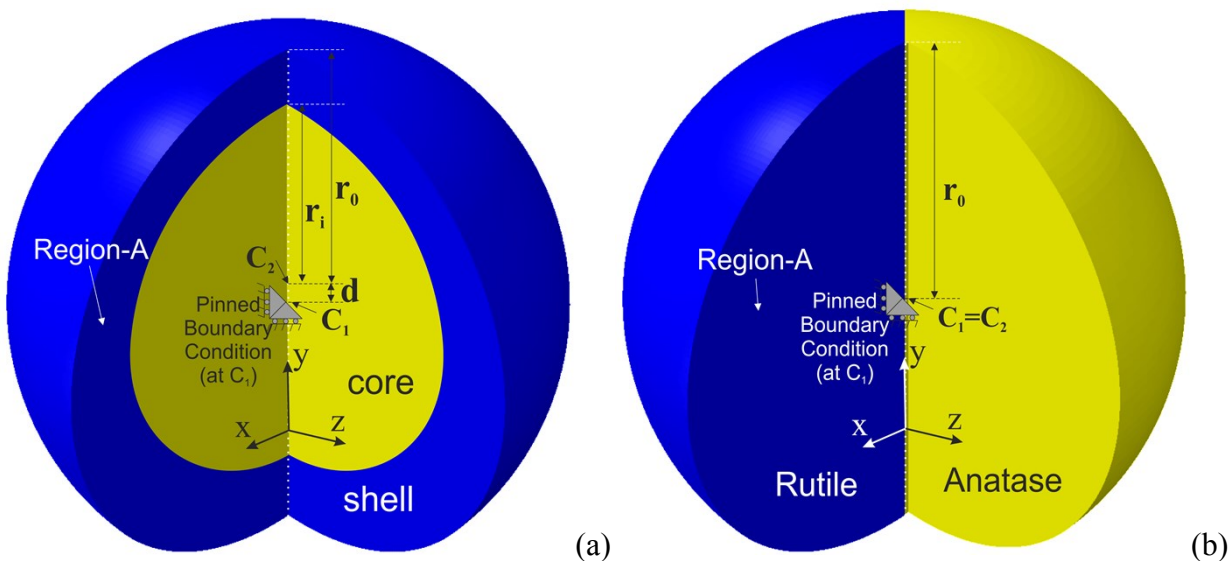


Figure S14. A schematic of the 3-dimensional finite element models (cut-section) used for the simulation of the stress state of: (a) core-shell and yolk heterostructures and (b) Janus heterostructures. The point C_1 is locked in x , y and z directions (pinned boundary condition at C_1). To compute the stress state of the coherent structures, eigenstrains are imposed as thermal strains in the regions highlighted with blue color (marked as region-A in both the parts). The volume of the phases is equal, while the outer radius r_0 is varied.

References

1. A. S. Barnard and P. Zapol, *Phys. Rev. B*, 2004, **70**, 235403.
2. A. Barnard and L. Curtiss, *Nano Lett.*, 2005, **5**, 1261-1266.
3. Z.-w. Qu and G.-J. Kroes, *J. Phys. Chem. B*, 2006, **110**, 8998-9007.
4. H. Zhang and J. F. Banfield, *J. Mater. Chem*, 1998, **8**, 2073-2076.